# Fibrinogen Patterns and Activity on Substrates with Tailored Hydroxy Density

José Carlos Rodríguez Hernández,[a] Patricia Rico,[a] David Moratal, Manuel Monleón Pradas, Manuel Salmerón-Sánchez*

The influence of the surface fraction of OH groups on fibrinogen (FG) adsorption is investigated in copolymers of ethyl acrylate and hydroxy ethylacrylate. The amount of adsorbed FG, quantified by western-blotting combined with image analysis of the corresponding bands, decreases as the hydrophilicity of the substrate increases. The influence of substrate wettability on FG conformation and distribution is observed by atomic force microscopy (AFM). The most hydrophobic substrate promotes FG fibrillogenesis, which leads to a fibrin-like appearance in the absence of any thrombin. The degree of FG interconnection was quantified by calculating the fractal dimension of the adsorbed protein from image analysis of the AFM results. The biological activity of the adsorbed FG is correlated to cell adhesion on FG-coated substrates.

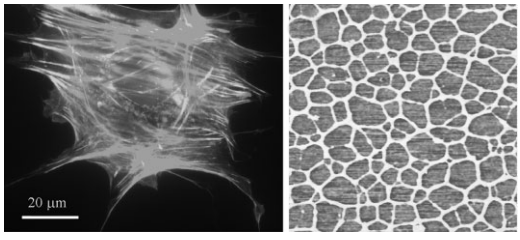


## Introduction

The biological response to a synthetic material depends on the concentration, distribution, and mobility of the protein layer that adsorbs upon contact with physiological fluids.[1,2] Protein adsorption on artificial substrates depends on the chemical groups of the substrate that determine the energetic (i.e., hydrogen bonding, electrostatic, van der Waals) and entropic interactions (the unfolding of the protein upon adsorption).[3–7] Among the several fibrous proteins involved in the cell–material interaction, this work is focused on fibrinogen (FG).

FG is a large, complex, fibrous glycoprotein normally present in human blood plasma essential for many biological functions which include haemostasis, wound healing, inflammation, and angiogenesis.[8] It is made up of three pairs of polypeptide chains, designated as A$\alpha$, B$\beta$, and $\gamma$, with molecular masses of 66, 52, and 46 kDa, respectively, which are held together by 29 disulfide bonds.[8] These six polypeptides are organized into independently folded units: a central E-domain, which includes the N-terminus of all six polypeptide chains, and two terminal D-domains, which include the B$\beta$ and $\gamma$ chains. The carboxy-terminal of the A$\alpha$ chain, the $\alpha$C-domain, departs from the D fragment and either associates to the E-domain to constitute a single globular domain close to it or, on the contrary, they form appendages with a certain degree of mobility. In its native form the $\alpha$C association to the central domain is more common; however, there is equilibrium between these two situations.[9] The cleavage of the small A and B sequences from the A$\alpha$ and B$\beta$ chains by thrombin in the E-domain yields fibrin, which is able to associate and polymerize. The length of an individual FG molecule is 45–50 nm.[10,11]

J. C. Rodríguez Hernández, P. Rico, D. Moratal, M. Monleón Pradas, M. Salmerón-Sánchez
Center for Biomaterials and Tissue Engineering, Universidad Politécnica de Valencia, 46022 Valencia, Spain
Fax: +34 963877276; E-mail: masalsan@fis.upv.es
M. Monleón Pradas, M. Salmerón-Sánchez
Regenerative Medicine Unit, Centro de Investigación Príncipe Felipe, Autopista del Saler 16, 46013 Valencia, Spain
J. C. Rodríguez Hernández, P. Rico, M. Monleón Pradas, M. Salmerón-Sánchez
Networking Research Center on Bioengineering, Biomaterials and Nanomedicine, CIBER-BBN, Valencia, Spain.

[a] These authors contributed equally to this work.


*Macromol. Biosci.* **2009**, *9*, 766–775

DOI: 10.1002/mabi.200800332

FG–surface interactions have been investigated on many substrates with different experimental techniques.[12] Atomic force microscopy (AFM), which is a technique able to provide direct observation of protein conformation on different substrates has been extensively used in recent years, mainly on model surfaces, such as silica, mica, titanium graphite, and self-assembled monolayers (SAMs), flat enough so that the height magnitude is able to reveal the trinodular structure of single-adsorbed FG molecules.[13–24]

The effect of surface wettability, as one of the most important parameters that affects the biological response to a material, on FG adsorption has lead to different, nonconsistent conclusions. Even if there is general agreement in the decrease of FG adsorption with the increase of wettability of the substrate,[25,26] it is not the case concerning FG conformation. Marchin et al. observed dramatic differences in the conformation of FG adsorbed on hydrophilic mica and hydrophobic graphite: globular conformations were observed on mica, whereas on graphite the trinodular structure of the extended molecule was clearly observed;[14] Sit et al. suggested that the spreading of FG increases with the hydrophobicity of the surface.[24] In addition, Wertz and Santore have shown through total internal reflection fluorescence that the footprint of a FG molecule is larger when adsorbed on a hydrophobic surface (graphite) than on a hydrophilic one (mica).[27,28] However, Agnihotri et al. found the trinodular conformation both on graphite and mica.[15]

The adhesion force between FG and the substrate has also been investigated by AFM and it has been found to depend on the surface wettability. By functionalizing AFM tips with the protein, Kidoaki et al. found that the strength of adhesion to a hydrophobic SAM was larger than to hydrophilic ones.[29] Xu et al. obtained adhesion forces to a series of surfaces over a broad wettability range through glow-discharge plasma modification, by using protein-modified AFM tips;[30] they showed a marked transition between protein adherent materials and protein nonadherent materials over the range of water contact angles of 60–65 °.

This work investigates FG adsorption on polymer hydrogels in which the surface density of hydroxy groups can be modulated as an independent parameter and, consequently, their wettability. The total amount of protein adsorbed on each substrate was quantified by a methodology that includes western-blotting combined with image analysis of the characteristic protein bands.[31] Moreover, the protein distribution on each surface was directly observed by making use of AFM. We demonstrate the substrate-induced fibrillogenesis of FG: we show and quantify (by means of image analysis of the AFM pictures) the formation of the protein network on the synthetic substrate induced solely by its surface chemistry. Finally, to show the influence of FG adsorption on the biological activity of the substrate, M3CT3 cell adhesion is investigated on the different FG-coated substrates.

## Experimental Part

### Preparation of Material Substrates

Copolymer sheets were obtained by polymerization of a solution of both monomers ethyl acrylate (EA, Aldrich, 99% pure) and hydroxyethyl acrylate (HEA, Aldrich 96% pure), with the desired proportion, using 0.1 wt.-% of benzoin (Scharlau, 98% pure) as photoinitiator and 2 wt.-% of ethyleneglycol dimethacrylate (EGDMA, Aldrich, 98% pure) as crosslinking agent. The polymerization was carried out up to limiting conversion. Five monomer feed compositions were chosen, given by the weight fraction of HEA in the initial mixture of 1, 0.7, 0.5, 0.3, and 0 (hereafter $OH_x$ will refer to the sample with percentage $x$ of HEA in the copolymer). After polymerization, low molecular mass substances were extracted from the material by boiling in ethanol for 24 h and then drying under vacuum to constant weight.

Small disks (approximately 5 mm in diameter) were cut from the polymerized plates in order to be used in the protein adsorption and cell adhesion studies. The samples were sterilized with gamma radiation (25 kGy) before the experiments.

### Swelling and Contact Angle Measurements

The equilibrium water content (mass of water absorbed referred to the dry mass of the substrate) and the water contact angle (determined using a Dataphysics OCA) were measured for the different substrates. Each experiment was performed in triplicate at room temperature.

### Atomic Force Microscopy (AFM)

Surfaces for AFM were prepared as follows. FG from human plasma (Sigma) was adsorbed on the different substrates by immersing the material disks in 20 $\mu g \cdot mL^{-1}$ physiological solution (0.9% NaCl) for 10 min. After that, the sample was dried by exposing its surface to a nitrogen flow for a few minutes. The influence of the concentration of the initial protein solution on the conformation of the adsorbed protein was investigated by immersing the pure PEA disk ($OH_0$) in protein solutions of different concentrations: 10, 14.3, 16.7, 20, 35, and 50 $\mu g \cdot mL^{-1}$. AFM was performed in a NanoScope III from Digital Instruments (Santa Barbara, CA) operating in the tapping mode in air; the Nanoscope 5.30r2 software version was used. Si-cantilevers from Veeco (Manchester, UK) were used with a force constant of 2.8 $N \cdot m^{-1}$ and a resonance frequency of 75 kHz. The phase signal was set to zero at a frequency 5–10% lower than the resonance one. Drive amplitude was 200 mV and the amplitude setpoint ($A_{sp}$) was 1.4 V. The ratio between the amplitude setpoint and the free amplitude ($A_{sp}/A_0$) was kept equal to 0.7.

The resistance of the adsorbed protein layer on the material surface was evaluated by performing extraction by detergents. Samples with adsorbed FG were washed in Laemmli buffer

($25 \times 10^{-3}$ M Tris, 2.5% sodium dodecyl sulfate (SDS), 10% glycerol, 0.1 $mg \cdot mL^{-1}$, 5% mercaptoethanol, and 6 M urea), rinsed in phosphate buffered saline (PBS), and observed again by AFM.

### Western-Blotting

Sample disks were placed in a 96-well tissue culture plate. FG from human plasma (Sigma) was adsorbed on the different substrates by immersing disks of the materials in a 20 $\mu g \cdot mL^{-1}$ physiological solution (0.9% NaCl) for 12 h at 37 °C.

Different aliquots of the non-adsorbed protein solution over the substrates were loaded into 5%-SDS polyacrylamide gel electrophoresis (PAGE). The samples were not boiled and no mercaptoethanol was added to the loading buffer ($25 \times 10^{-3}$ M Tris, 2.5% SDS, 10% glycerol, 0.1 $mg \cdot mL^{-1}$ bromophenol blue; pH 6.8) in order to avoid FG breakage. Proteins were transferred to a positively charged poly(vinylidene difluoride) nylon membrane (GE Healthcare) using a semidry transfer cell system (Biorad), and blocked by immersion in 5% skimmed milk in PBS for 1 h at room temperature. The blot was incubated with monoclonal anti-human FG clone FG-21 antibody (developed in mouse, Sigma) (1:500) in PBS that contained 0.1% TWEEN 20 (a polysorbate surfactant commonly used as a blocking agent and washing solution in Western blot) and 2% skimmed milk for 1 h at room temperature and washed three times (10 min for each wash) with PBS that contained 0.1% TWEEN 20. The blot was subsequently incubated in horseradish peroxidase-conjugated goat anti-mouse immunoglobulin G (GE Healthcare) diluted 1: 5 000 in PBS that contained TWEEN 20 and 2% milk (1 h at room temperature).

An enhanced chemiluminescence detection system (GE Healthcare) was used according to the manufacturer's instructions prior to exposing the blot to X-ray film for 1 min.

### Image Processing

All image processing and analysis was done using self-developed software developed under MATLAB R2006a (The MathWorks, Inc., Natick, MA, USA).

All the western blotting bands were digitized using the same scanner (Epson Stylus Photo RX500, Seiko Epson Corp., Nagano, Japan) and the same scan parameters: 8 bits gray scale image and 300 dots per inch. The digitized images were binarized using the Otsu's method,[32] which chooses the threshold that minimizes the intraclass variance of the thresholded black and white pixels, in order to create a mask that automatically selected the edge of each western blot band. This mask was applied to a negative version of the original scanned picture to provide an image that contained only the western bands. The last step of the process consisted finally in adding all the pixels that confirmed each band correctly weighted by their intensity level.

The degree of connectivity of the protein adsorbed on the substrate was studied using fractal techniques. Our fractal analysis was based on the calculation of the fractal dimension parameter ($D$) of each image using the box-counting algorithm that consisted of superposing a grid of square edge $\lambda$ on the image and counting the squares that contained boundaries ($N$); this process was repeated with other values of square edge.[33] Different values of the ratio ln ($N$)/ln ($\lambda$) were obtained to determine a straight line whose slope $m$ is related to the fractal dimension by $D = -m$.[33,34] Before applying the box-counting algorithm, the image was gray-scaled and binarized using the Otsu's method. The contour of the protein was automatically detected in this binarized version of the image and finally the fractal dimension was calculated on this image by applying the box-counting algorithm.

### Cell Culture

MC3T3-E1 cells were obtained from the RIKEN CELL BANK (Japan). Prior to seeding on FG-coated substrates, cells were maintained in DMEM medium supplemented with 10% foetal bovine serum and 1% penicillin-streptomycin and passaged twice a week using standard techniques.

Sample disks (5 mm in diameter) placed in a 96-well tissue culture plate were coated with 20 $\mu g \cdot mL^{-1}$ of FG (12 h at 37 °C). Cells ($10^4$) were then placed onto each substrate and were maintained at 37 °C in a humidified atmosphere under 5% $CO_2$ for 3 h. Each experiment was performed in triplicate.

After 3 h of culture, MC3T3-E1 cells were washed in Dulbecco's phosphate buffered saline (DPBS, Invitrogen) and fixed in Formalin solution 10% (Sigma) at 4 °C for 1 h. Afterwards, the samples were rinsed with DPBS and a permeabilising buffer (10.3 g sucrose, 0.292 g NaCl, 0.06 g $MgCl_2$, 0.476 g Hepes buffer, 0.5 mL of Triton X, in 100 mL water, pH 7.2) was added at room temperature for 5 min. In order to reduce the background signal, the samples were then incubated in 2% BSA (bovine serum albumin)/DPBS at room temperature with BODIPY FL phallacidin (2–3 units per sample, Molecular Probes). The samples were then rinsed in DPBS three times for 5 min each. Finally, samples were washed before being mounted in a Vectashield that contained DAPI staining (Vector Laboratories). A Leica DM6000B fluorescent microscope was used. The image system was equipped with a Leica DFC350FX camera.

## Results And Discussion

### Protein Quantification by Western-Blotting

Figure 1 shows the calibration procedure employed to quantify FG adsorption by western-blotting. Gels were loaded with known amounts of FG (Figure 1a) and the resulting bands were quantified by image analysis making use of the Otsu's algorithm to systematically identify the band borders (Figure 1b).[32] The algorithm developed allows identification of the contour of the band independently of the user. Band intensity increases as the protein concentration does, and it is unequivocally correlated to FG amount, which allows one to build a calibration curve (Figure 1c). The calibration curve shows a linear correlation between intensities and FG mass from 200 ng on, a value that can be taken as the lower sensitivity limit of the technique for this protein.


Macromol. Biosci. 2009, 9, 766–775

Macromolecular Journals
DOI: 10.1002/mabi.200800332

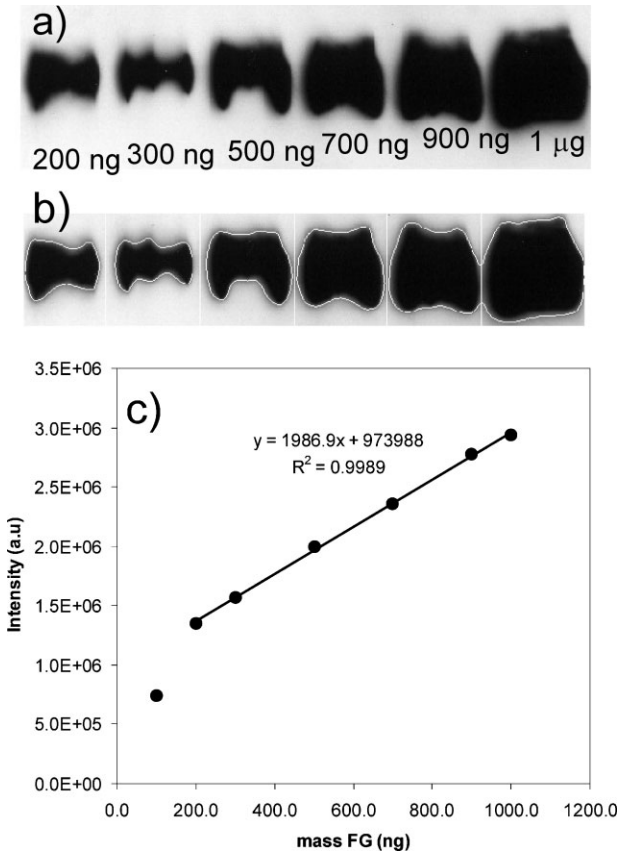


*Figure 1.* Western-blot bands with increasing FG loads (a), its systematic border definition (b), and the resulting calibration curve (c). The straight line is a linear regression of the data in the sensitivity range of the technique.

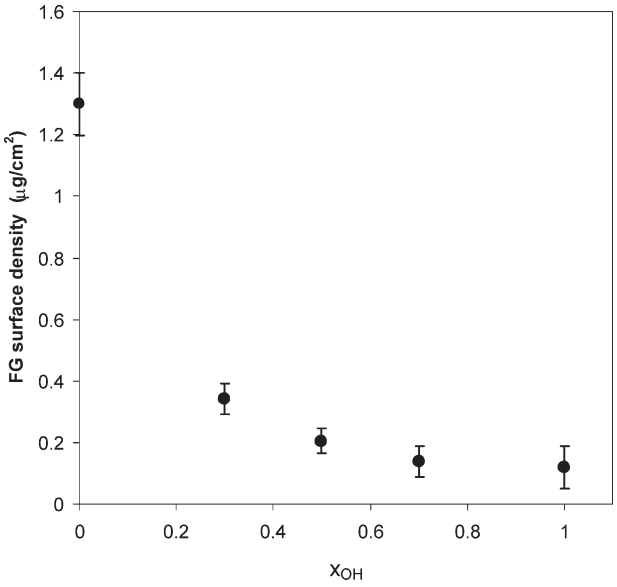


*Figure 2.* FG adsorption versus hydroxy surface density ($x_{OH}$). Adsorption was done from a 20 $\mu g \cdot mL^{-1}$ solution of FG in physiological solution (0.9% NaCl). Error bars are the standard deviations for three measurements.

The calibration procedure has been used to quantify the amount of FG adsorbed on the different substrates. Each experiment included two calibration points so that the position of the whole calibration curve could be checked each time. Figure 2 shows the results of the experiment after immersing the different substrates in 20 $\mu g \cdot mL^{-1}$ physiological solution (0.9% NaCl) for 12 h. The amount of adsorbed protein diminishes monotonically as the OH density increases. The difference of adsorbed FG between pure PEA ($OH_0$) and $OH_{30}$ is approx. 0.9 $\mu g \cdot cm^{-2}$, a huge fall for such a small OH increment, whereas these differences tend to diminish as substrata become more hydrophilic (<0.1 $\mu g \cdot cm^{-2}$).

## FG Adsorption by AFM

Figure 3 shows AFM phase images showing the FG conformation on the most hydrophobic substratum (pure PEA, $OH_0$) after adsorption from protein solutions of different concentrations for 10 min. Up to protein solution concentrations of 14.3 $\mu g \cdot mL^{-1}$, single FG molecules in globular conformations are observed (Figure 3a,b). However, from this concentration on, protein–protein interactions are enhanced and FG clusters with elongated shapes begin to form (Figure 3c). With a further increase of protein concentration in the solution (>16.7 $\mu g \cdot mL^{-1}$), FG fibrillar structures interact and eventually a well-defined protein network arises (Figure 3d). The average strut thickness of the network depends on the FG solution concentration (Figure 3e,f).

Network formation was studied by image analysis of sets of $2 \times 2$ $\mu m^2$ AFM images (Figure 3g–l): the fractal dimension (*D*), a parameter that accounts for the network connectivity, as well as the area fraction of the image covered by the protein were determined (Figure 4). The fractal dimension increases as the concentration of the solution does until a threshold is reached (≈20 $\mu g \cdot mL^{-1}$) at which struts begin to thicken and small network features tend to vanish, which leads to some decrease in *D*. In addition, the fraction of the image covered by FG increases monotonically with protein concentration in the solution up to saturation (≈35 $\mu g \cdot mL^{-1}$).

Figure 5 shows FG distribution after adsorption on the different substrata at different magnifications from a 20 $\mu g \cdot mL^{-1}$ protein solution, which is the concentration afterwards employed to coat the substrates with the protein for cell culture purposes. This protein concentration does not reveal the conformation of single FG proteins since FG fibrils are present in all samples: rather than single FG molecules, AFM images show protein patterns with different topologies. Nevertheless, some differences

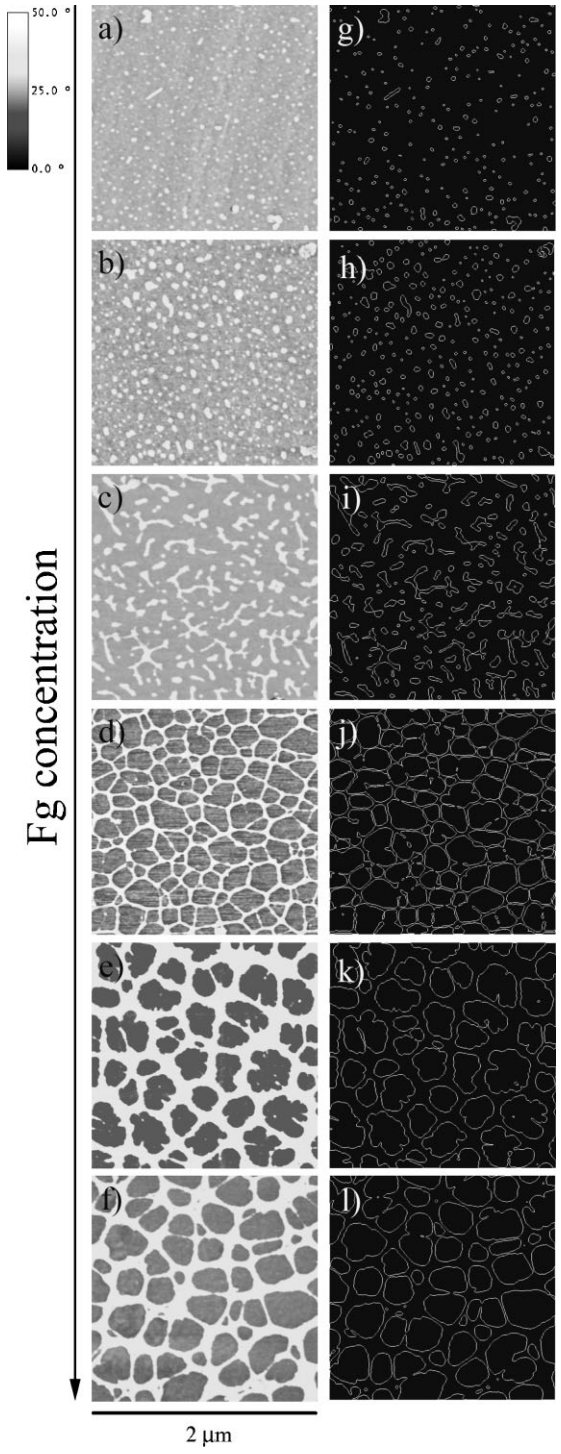


*Figure 3.* Phase signal AFM images of the formation of a FG network on pure PEA ($OH_o$) at a fixed immersion time (10 min) and different protein concentrations: a) 10, b) 14.3, c) 16.7, d) 20, e) 35, and f) 50 $\mu g \cdot mL^{-1}$. Opposite each AFM image is the binarized image employed to compute the topologic network parameters (fractal dimension). The scale bar is common for all AFM images.

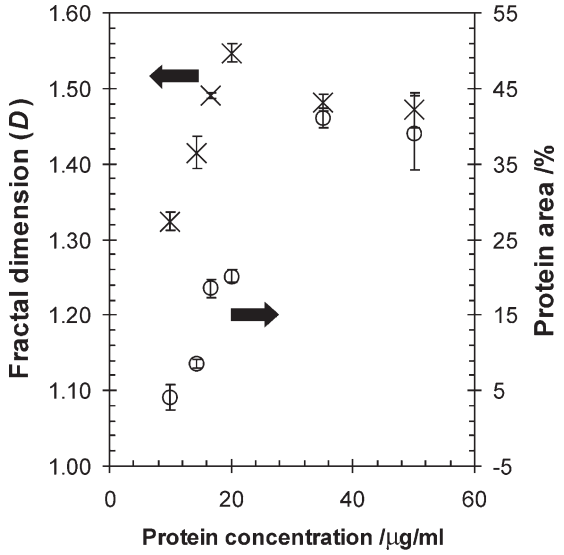


*Figure 4.* Fractal dimension (*x*) and percentage of the area covered by FG (o) after immersions at different feed protein concentrations. Error bars are the standard deviations of at least three different 2 × 2 $\mu m^2$ AFM phase images.

between the conformations of FG on the different substrates are worth mentioning. The formation of a FG network takes place on pure PEA ($OH_0$), but the co-continuity of the protein network is lost when small amounts of OH are introduced in the system ($OH_{10}$ and $OH_{20}$ Figure 5b,c). However, from this hydroxy content on, FG–FG interactions are somehow enhanced and variable fibril network topologies show up again (Figure 5d–g).

The evolution of the fractal dimension *D* with the hydroxy density in the substrate is shown in Figure 6. The interconnectivity of the FG network observed on pure PEA and PHEA ($OH_0$ and $OH_{100}$, respectively) is similar even though the protein networks look qualitatively different from AFM images (Figure 5a and g). Moreover, the interconnection degree diminishes for intermediate fractions of hydroxy groups in the system.

Figure 7 shows the surfaces of samples after washing the adsorbed FG with the most commonly used buffer for protein extraction (Laemmli buffer). It can be observed that the self-assembled network on the most hydrophobic substrate ($OH_0$) cannot withstand the extraction by detergents and only dispersed aggregates remain on the surface (Figure 7a). Protein aggregates are also observed on the $OH_{100}$ substrate after detergent extraction (Figure 7c) in contrast to the initially observed network (Figure 5g). However, on samples with intermediate composition (e.g., $OH_{50}$) initial protein aggregates (Figure 5c) are completely extracted by the detergent and the nude surface, without any trace of the protein, is observed in Figure 7b.


*Macromol. Biosci.* **2009**, *9*, 766–775

Macromolecular Journals
DOI: 10.1002/mabi.200800332

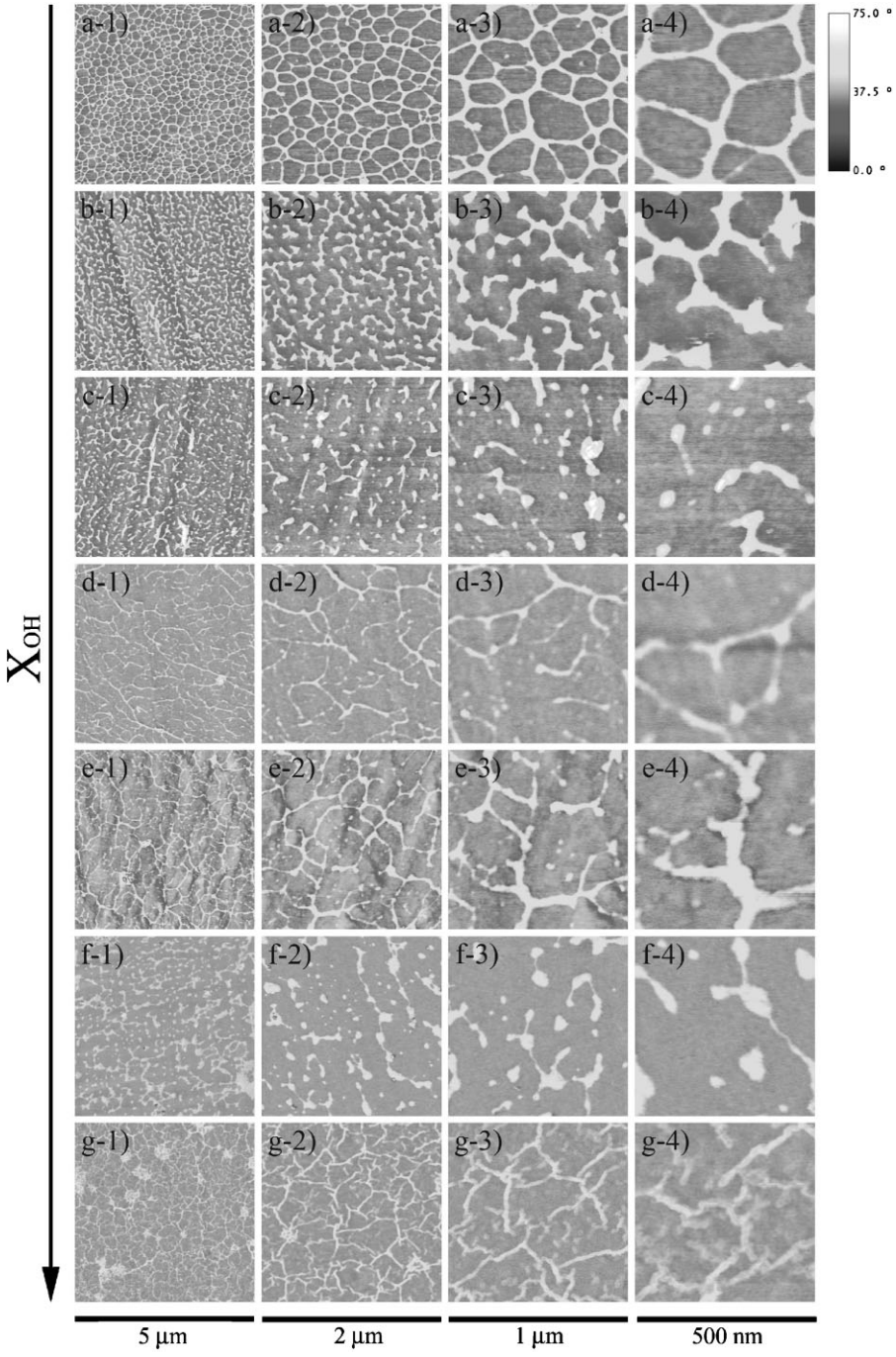


*Figure 5.* Phase signal AFM images after FG adsorption on substrates with controlled hydroxy surface densities ($x_{OH}$): a) pure PEA ($OH_0$), b) $OH_{10}$, c) $OH_{20}$, d) $OH_{30}$, e) $OH_{50}$, f) $OH_{70}$, g) and pure PHEA ($OH_{100}$). The scale bar is common for all images.

## Biological Activity

Substrates were immersed overnight in a FG solution (20 μg · $mL^{-1}$) prior to cell culture. The F-actin cytoskeleton formation was examined after 3 h of cell culture. The state of the actin cytoskeleton depended strongly on the amount of OH groups in the samples. On the more hydrophobic polymers ($OH_0$ and $OH_{30}$), cells spread on the surface with a well-defined and developed F-actin cytoskeleton (Figure 8a and c), which leads to the formation of well-defined focal adhesions as observed by vinculin immunodetection (Figure 8b). Higher fractions of hydroxy groups in the substrate lead to a less spread morphology and only initial-peripheric trends of F-actin are visible ($OH_{50}$, Figure 8d). Moreover, from this OH content on, i.e., for the most wettable substrates ($OH_{70}$ and $OH_{100}$), cells show rounded shapes with no trace of a well-developed F-actin cytoskeleton (Figure 8e and f). The viability of cells on $OH_{70}$ and $OH_{100}$ was assessed by collecting cells after 3 h of culture and seeding them on control TCPS plates, where they adhered and expanded normally.

Cells were cultured for 1 h to gain further insight into the direct effects of FG on cell attachment and spreading. Figure 9 shows the different cell morphology between cells on $OH_0$, $OH_{30}$, and $OH_{50}$. Clearly, F-actin cytoskeleton formation is faster on $OH_0$, with well-develop fibers after 1 h, and it is delayed as wettability increases.

## General Discussion

The distribution, conformation, and mobility of a protein and the strength of its interaction with the substrate must be taken into account to understand protein adsorption on a synthetic surface and the ensuing biological response of the material.[35,36] It is well known that these phenomena are strongly influenced by the surface properties of the material, in particular the wettability of the surface.[36–41] The copolymer substrates employed in this work are based on the random combination of EA and HEA monomers, which have a vinyl backbone chain with the side groups $-COOCH_2CH_3$ and $-COOCH_2CH_2OH$, respectively. Their copolymeriza-

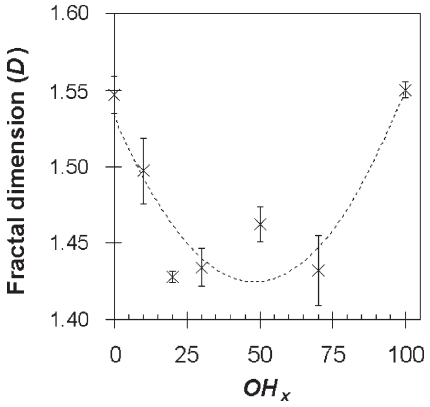


*Figure 6.* Hydroxy density dependence of the fractal dimension (*D*). Error bars are the standard deviations for at least three different AFM images of $2 \times 2$ μm$^2$. A two-order polynomial regression (dotted line) is represented as a guide to the eye.

tion gives rise to a substrate in which the surface density of OH groups can be varied without modifying any other chemical functionality of the system. Our substrates were sheets of approx. 1 mm thickness in the rubber state (room temperature is well-above the glass transition temperature), so their moduli are that of an elastomer (approx. 1 MPa, independent of composition).[42] The concentration of OH groups determines both the wettability and the hydrophilicity of the substrate, while the surface roughness remains unaffected (Table 1). The interaction of the protein domains with the chemical functionalities of the substrate and with water determines the molecule's adsorbed conformations as well as the amount of adsorbed protein.

AFM studies of the adsorption of protein on non-model surfaces in cases where the roughness of the substrate is of a size of the order of the protein height cannot be conclusive if monitored with the height signal since the protein features are usually blurred; one would have to polish the neat material to get a surface flat enough.[43] Instead of the height, the phase signal of AFM, which is a magnitude sensitive to the different viscoelastic behaviors,[44–47] can be used to distinctly reveal protein conformation under conditions of usual, non-model

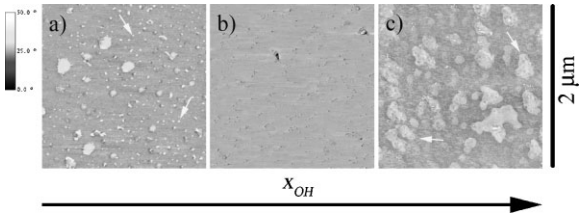


*Figure 7.* FG resistance to extraction by detergents. Phase signal AFM images show the sample substrates after washing with Laemmli buffer: a) pure PEA ($OH_o$), b) $OH_{50}$, c) pure PHEA ($OH_{100}$). Arrows point to protein clusters after the extraction procedure.

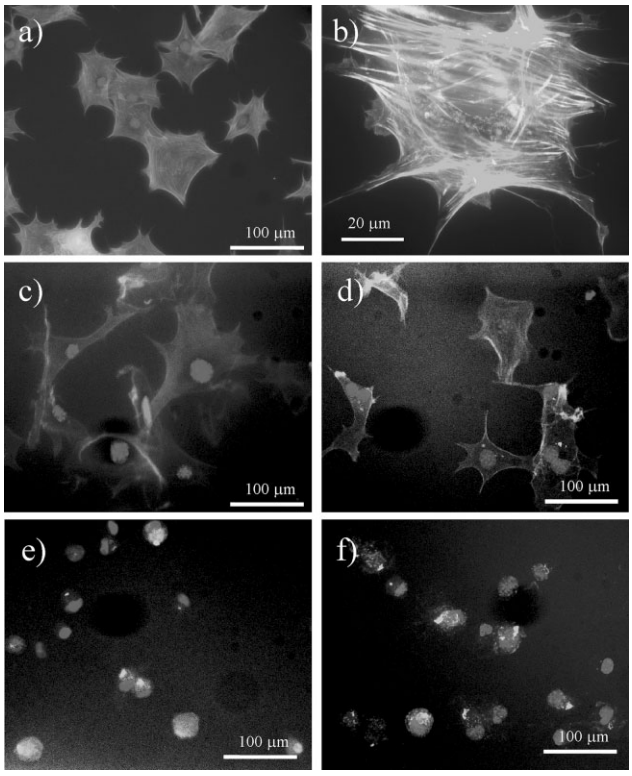


*Figure 8.* F-actin cytoskeleton after 3 h of culture on substrates with increasing fraction of hydroxy groups. a,b) pure PEA ($OH_o$), c) $OH_{30}$, d) $OH_{50}$, e) $OH_{70}$, and (f) pure PHEA ($OH_{100}$). Nuclei were counterstained with DAPI. Image (b) shows focal adhesion protein vinculin.

polymer surfaces.[48,49] The phase magnitude (Figure 5) as well as the fractal dimension *D* calculated from image analysis (Figure 6) reveal that only on the most hydrophobic and hydrophilic substrates ($OH_0$ and $OH_{100}$, respectively), is a well-connected protein network formed on the surface. Nevertheless, the conformation of the FG must be different, since the biological activity of the FG-coated substrates is very different: cells spread on the hydrophobic substrate showing excellent adhesion, but rounded cells are found on the hydrophilic one (Figure 8). It has been shown that, excluding platelets that interact with the C-terminal region of the FG $\gamma$-chain by the $\alpha_{IIb}\beta_3$

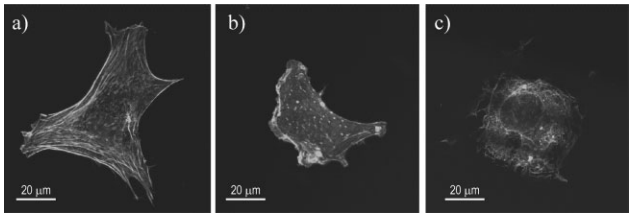


*Figure 9.* F-actin cytoskeleton after 1 h of culture on substrates with increasing fraction of hydroxy groups. a) pure PEA ($OH_o$), b) $OH_{30}$, c) and $OH_{50}$. Nuclei were counterstained with DAPI.


*Macromol. Biosci.* **2009**, *9*, 766–775

Macromolecular Journals

DOI: 10.1002/mabi.200800332

*Table 1.* Equilibrium water content (EWC) and water contact angle (WCA) for the different substrates. Mean values and their standard deviations are reported for both EWC and WCA. The last two columns show the roughness parameters ($R_{max}$: the difference between the highest and lowest heights; RMS: root mean square, the standard deviation of the height values) for the different samples calculated on $1 \times 1\ \mu m^2$ before FG adsorption.

| $x_{OH}$ | EWC | WCA | $R_{max}$ | RMS |
|---|---|---|---|---|
| | | deg. | nm | nm |
| 0 | $1.7 \pm 0.4$ | $89 \pm 1$ | 24.3 | 3.1 |
| 0.3 | $7.6 \pm 0.9$ | $80 \pm 2$ | 8.5 | 1.5 |
| 0.5 | $18.2 \pm 1.7$ | $67 \pm 1$ | 10.6 | 1.1 |
| 0.7 | $40.6 \pm 0.4$ | $55 \pm 1$ | 17.1 | 1.5 |
| 1 | $134 \pm 5$ | $45 \pm 2$ | 6.9 | 1.2 |

integrin receptor,[50] cell adhesion to FG is mediated by the $\alpha_v\beta_3$ integrin, which recognizes the RGD sequence near the C-terminus of the A$\alpha$ chain of the FG molecules (RGDF at A$\alpha$95–98 and RGDS at A$\alpha$572–575).[51–54] Our results suggest conformations of the adsorbed FG that lead to the recognition of the RGD sequence by integrins on the most hydrophobic substrates, while on the more hydrophilic surfaces the conformation of the A$\alpha$ chain, which hides the RGD sequence, prevents cell adhesion (Figure 8). Moreover, the amount of FG adsorbed on $OH_{100}$ is much lower than that on the hydrophobic $OH_0$ (Figure 2). The decrease in FG adsorption as the wettability of the substrate increases has been pointed out in the literature.[25,26]

Gettens et al. observed the formation of a FG network on a graphite surface when adsorbing from protein solutions of concentrations higher than 5 $\mu g \cdot mL^{-1}$ for 60 min, but not on mica.[18] Assuming that each protein aggregates as a side-on packed monolayer with a surface density of 2.1 $mg \cdot m^{-2}$,[18] then the upper value of the protein concentration for a 45% surface coverage (Figure 4) is 1 $mg \cdot m^{-2}$, an order of magnitude below the equilibrium value quantified by western-blot (Figure 2). This result, in agreement with Toscano and Santore,[13,55] indicates that even when the AFM images may appear full at relatively short times, they actually contain only about 10% of their protein capacity.[55] FG network formation on our substrates have patterns similar to those found by Gettens et al. on graphite and to those observed by Sit and Marchant in the process of fibrin assembly on graphite in the presence of thrombin.[18,56] The formation of the network structure even in the absence of any thrombin suggests a specific interaction between FG molecules. One reported way to establish intermolecular interactions between FG molecules implies electrostatic bonds between those globular $\alpha$C-termini (which are negatively charged) and the overall positive charge of the E domain.[13] Likewise, $\alpha$C-termini are also able to bind themselves as demonstrated by the work developed by Veklich et al.[9] Fibrillogenesis, the formation of a fibrillar-like structure of the protein, has also been described as a process driven by cells which occurs when integrins interact with the adequate domains of the fibronectin protein and extend their subunits to give rise to the formation of a network of fibrils.[57] Our results show that this process can take place as a consequence of the sole interaction between the protein molecules and a material surface, i.e., without the need of either thrombin or cell involvement. Nevertheless, the interaction between this FG network and the substrate is not strong enough so as to resist extraction by detergents (Figure 7a).

On the surfaces with intermediate fractions of OH groups, formation of a protein network does not take place (Figure 5), as indicated by the minimum in the curve of the fractal dimension $D$ (Figure 6). FG aggregation still occurs on these substrates, which suggests that FG–FG interactions continue but, since the amount of protein adsorbed decreases as the wettability of the surface increases (Figure 3), a complete coverage of the surface does not happen anymore. FG conformation on the substrate is not directly related to the total amount of protein adsorbed on it. If protein adsorption on a substrate's surface is analyzed in terms of the number of available sites on the surface, it is clear that not only the energetic interactions between the substrate and the protein play a role in the adsorption process, but also the conformation of the protein, the configurational entropy, must control the amount of molecules directly adsorbed on the substrate. It has been found that the footprint of a FG molecule is larger when adsorbed on a hydrophobic surface than on a hydrophilic one,[27,28] and higher amounts of adsorbed proteins on the most hydrophobic surface result in an ordered FG–FG adsorption, which leads to the formation of a network on the substrate. As hydrophilicity increases, the amount of FG directly in contact with the substrate decreases, as well as the footprint of the molecule, which results in the formation of isolated FG aggregates (Figure 5). In addition, these isolated aggregates are completely extracted by detergents and no trace of protein is found on the material surface after washing (Figure 7b). Nevertheless, cell adhesion to the substrates that contain up to 50% hydroxy groups ($OH_0$, $OH_{30}$, $OH_{50}$) is accompanied by the formation of the actin cytoskeleton and a spread morphology, which suggests that the conformation of the protein is still adequate to enhance the cell–FG interaction, even if the number of cells adhered on the substrate is lower once the co-continuity of the FG network is lost (Figure 8). Nevertheless, there is a strong influence of FG adsorption on the initial interaction (after 1 h) on the different surfaces (Figure 9): cell spreading and F-actin cytoskeleton formation is faster on the most hydrophobic substrate.

Even if the cell behavior is qualitatively the same on these three substrates after 3 h, the initial cell adhesion and spread is faster the lower the amount of OH groups in the substrate (Figure 9). This suggests that the initial cell–FG interaction is enhanced on $OH_0$ but, after 3 h, cells seeded on $OH_{30}$ and $OH_{50}$ are able to overcome the initial situation, probably by producing their own matrix at the material interface.[35,36]

Higher amounts of hydroxy groups in the substrate (samples $OH_{70}$ and $OH_{100}$) result in a qualitative change of the cell–material interaction: cells hardly adhere on the substrate, and show a rounded morphology and lack of focal adhesion contacts and actin cytoskeleton. Since the amount of adsorbed FG at these higher contents of hydroxy groups in the substrate is only slightly lower, we must ascribe this behavior to the different conformation of the protein on the substrate, which results in non-accessible RGD domains able to promote the integrin linking. Of interest is the formation of a FG network on the most hydrophilic substrate. Taking into account the monotonic decrease of the amount of adsorbed protein with substrate's hydrophilicity (Figure 2) we cannot discard that the formation of FG aggregates in $OH_{100}$ is a consequence of the drying process, which could lead to lateral reorganization of the adsorbed layer at the air–liquid interface; this process seems to be favored on very hydrophilic surfaces because of the absence of FG–surface interactions strong enough to prevent protein relaxation during water release.[22]

## Conclusion

The amount of FG adsorbed on substrates with controlled hydroxy fraction decreases as the wettability of the substrate increases. The formation of a FG network is revealed on the most hydrophobic substrate, on which FG–FG interactions are enhanced, in a protein conformation such that the RGD domains are recognized by cells and lead to excellent cell adhesion. Higher amounts of hydroxy densities result in the formation of FG aggregates on the substrates but lack protein co-continuity on the surface. Nevertheless, for these intermediate hydroxy surfaces, there is a qualitative change in FG conformation, which results in a lack of cell adhesion to the substrate.

Acknowledgements: AFM was performed under the technical guidance of the *Microscopy Service at the Universidad Politécnica de Valencia*, whose advice is greatly appreciated. The confocal microscopic work has been done by the *Confocal Microscopy Service of the Centro de Investigación Principe Felipe* (Valencia, Spain). The support of the *Spanish Ministry of Science* through project No. MAT2006-08120 (including the FEDER financial support) is kindly acknowledged.

Received: November 12, 2008; Revised: February 11, 2009; Accepted: February 16, 2009; DOI: 10.1002/mabi.200800332

Keywords: atomic force microscopy; cell-material interaction; fibrinogen; proteins

[1] B. M. Gumbiner, *Cell* **1996**, *84*, 345.
[2] K. Anselme, *Biomaterials* **2000**, *21*, 667.
[3] A. J. García, *Adv. Polym. Sci.* **2006**, *203*, 171.
[4] C. Werner, T. Pompe, K. Salchert, *Adv. Polym. Sci.* **2006**, *203*, 63.
[5] B. G. Keselowsky, D. M. Collard, A. J. García, *J. Biomed. Mater. Res. A* **2003**, *66*, 247.
[6] K. E. Michael, V. N. Vernekar, B. G. Keselowsky, J. C. Meredith, R. A. Latoru, A. J. García, *Langmuir* **2003**, *19*, 8033.
[7] T. S. Tsapikouni, Y. F. Missirlis, *Colloids Surf. B* **2007**, *57*, 89.
[8] J. W. Weisel, *Adv. Prot. Chem.* **2005**, *70*, 2497.
[9] Y. I. Veklich, O. V. Gorkun, L. V. Medved, W. Nieuwenhuizen, J. W. Weisel, *J. Biol. Chem.* **1993**, *268*, 13577.
[10] J. W. Weisel, C. V. Stauffacher, E. Bullitt, C. Cohen, *Science* **1985**, *230*, 1388.
[11] R. R. Gorman, G. E. Stoner, A. Catlin, *J. Phys. Chem.* **1971**, *75*, 2103.
[12] J. L. Brash, T. A. Horbett, "Protein at Interfaces II: Fundamentals and Applications", in: *ACS Symposium Series No. 602*, J. L. Brash, T. A. Horbett, Eds., American Chemical Society, Washington, DC 1995, Chapter 1.
[13] A. Toscano, M. Santore, *Langmuir* **2006**, *22*, 2588.
[14] K. L. Marchin, C. L. Berrie, *Langmuir* **2003**, *19*, 9883.
[15] A. Agnihotri, C. A. Siedlecki, *Langmuir* **2004**, *20*, 8846.
[16] P. Cacciafesta, A. D. L. Humphris, K. D. Jandt, M. J. Miles, *Langmuir* **2000**, *16*, 8167.
[17] S. Tunc, M. F. Maitz, G. Steiner, L. Vázquez, M. T. Pham, R. Salzer, *Colloids Surf. B* **2005**, *42*, 219.
[18] R. T. T. Gettens, Z. Bai, J. L. Gilbert, *J. Biomed. Mater. Res. A* **2005**, *72*, 246.
[19] R. T. T. Gettens, J. L. Gilbert, *J. Biomed. Mater. Res. A* **2007**, *81*, 465.
[20] T. C. Ta, M. McDermott, *Anal. Chem.* **2000**, *72*, 2627.
[21] T. Ishizaki, N. Saito, Y. Sato, O. Takai, *Surf. Sci.* **2007**, *601*, 3861.
[22] J. L. Ortega-Vinuesa, P. Tengvall, I. Lundström, *J. Colloid Interface Sci.* **1998**, *207*, 228.
[23] K. Mitsakakis, S. Lousinian, S. Logothetidis, *Biomol. Eng.* **2007**, *24*, 119.
[24] P. S. Sit, R. E. Marchant, *Thromb. Haemost.* **1999**, *82*, 1053.
[25] S. M. Slack, T. A. Horbett, *J. Biomed. Mater. Res.* **1992**, *26*, 1633.
[26] S. N. Rodrigues, I. C. Gonçalves, M. C. L. Martins, M. A. Barbosa, B. Ratner, *Biomaterials* **2006**, *27*, 5357.
[27] C. F. Wertz, M. M. Santore, *Langmuir* **2001**, *17*, 3006.
[28] C. F. Wertz, M. M. Santore, *Langmuir* **2002**, *18*, 706.
[29] S. Kidoaki, T. Matsuda, *Langmuir* **1999**, *15*, 7639.
[30] L.-C. Xu, C. A. Siedlecki, *Biomaterials* **2007**, *28*, 3273.
[31] D. Gugutkov, G. Altankov, J. C. Rodríguez Hernández, M. Monleón Pradas, M. Salmerón-Sánchez, *J. Biomed. Mater. Res. A.* **2009**, in press. DOI: 10.1002/jbm.a.32374
[32] N. Otsu, *IEEE Trans. Syst. Man. Cybern.* **1979**, *9*, 62.
[33] J. M. Keller, S. Chen, R. M. Crownover, *Computer Vision, Graphics, and Image Processing* **1989**, *45*, 150.
[34] L. Pothuaud, C. L. Benhamou, P. Porion, E. Lespessailles, R. Harba, P. Levitz, *J. Bone Mineral. Res.* **2000**, *15*, 691.
[35] G. Altankov, T. Groth, *J. Mater. Sci. Mater. Med.* **1994**, *5*, 732.
[36] G. Altankov, T. Groth, *J. Mater. Sci. Mater. Med.* **1996**, *7*, 425.
[37] A. J. García, D. B. Boettiger, *Biomaterials* **1999**, *20*, 2427.




DOI: 10.1002/mabi.200800332

[38] G. K. Toworfe, R. J. Composto, C. S. Adams, I. M. Shapiro, P. Ducheyne, *J. Biomed. Mater. Res. A* **2004**, *71*, 449.
[39] L. Baugh, L. Vogel, *J. Biomed. Mater. Res. A* **2004**, *69*, 525.
[40] M. A. Lan, C. A. Gersbach, K. E. Michael, B. G. Keselowsky, A. J. García, *Biomaterials* **2005**, *26*, 4523.
[41] F. Grinnell, M. K. Feld, *J. Biol. Chem.* **1982**, *257*, 4888.
[42] A. Campillo Fernández, M. Salmerón Sánchez, R. Sabater i Serra, J. M. Meseguer Dueñas, J. L. Gómez Ribelles, *Eur. Polym. J.* **2003**, *44*, 1996.
[43] I. Van De Keere, R. Willaert, A. Hubin, J. Vereecken, *Langmuir* **2008**, *24*, 1844.
[44] J. Tamayo, R. García, *Appl. Phys. Lett.* **1997**, *71*, 2394.
[45] J. P. Cleveland, B. Anczykowski, A. E. Schmid, V. B. Elings, *Appl. Phys. Lett.* **1998**, *72*, 2613.
[46] J. Tamayo, R. García, *Appl. Phys. Lett.* **1998**, *73*, 2926.
[47] R. García, J. Tamayo, M. Calleja, F. García, *Appl. Phys. A* **1998**, *66*, S309.
[48] N. B. Holland, R. E. Marchant, *Biomed. Mater. Res. A* **2000**, *51*, 307.
[49] J. C. Rodríguez Hernández, M. Salmerón Sánchez, J. M. Soria, J. L. Gómez Ribelles, M. Monleon Pradas, *Biophys. J.* **2007**, *93*, 202.
[50] D. H. Farell, P. Thiagarajan, D. W. Chung, E. W. Davie, *Proc. Natl. Acad. Sci.* **1992**, *89*, 10729.
[51] D. Cheresh, *Proc. Natl. Acad. Sci.* **1987**, *84*, 6471.
[52] D. Cheresh, S. Berliner, V. Vicente, Z. Ruggery, *Cell* **1989**, *58*, 945.
[53] F. Gailit, C. Clarke, D. Newman, M. G. Tonnesen, M. W. Mosesson, R. A. F. Clark, *Exp. Cell. Res.* **1997**, *232*, 118.
[54] R. F. Doolittle, K. W. K. Watt, B. A. Cottrell, D. D. Strong, M. Riley, *Nature* **1979**, *280*, 464.
[55] C. F. Wertz, M. M. Santore, *Langmuir* **1999**, *15*, 8884.
[56] P. S. Sit, R. E. Marchant, *Surf. Sci.* **2001**, *491*, 421.
[57] R. Tzoneva, T. Groth, G. Altankov, D. Paul, *J. Mater. Sci. Mater. Med.* **2002**, *13*, 425.